

Annexes and Tables

Summary. This chapter features solutions to selected exercises, some pictures chosen from the online database of all profiles of pc-sets <http://canonsrythmiques.free.fr/MaRecherche/photos-2/> which have been included here because they are mentioned in the main text, and, for reference, tables of singular pc-sets, phases of triads, enumeration of the most symmetrically pc-sets in the sense of Proposition 6.10, and values of Major Scale Similarity for a large panel of historical temperaments.

8.1 Solutions to some exercises

1.39 All sums run over the whole \mathbb{Z}_n :

$$\begin{aligned} \widehat{f * g}(x) &= \sum_k (f * g(k)) e^{-2i\pi kx/n} = \sum_k \sum_j f(k-j)g(j) e^{-2i\pi(k-j+j)x/n} \\ &= \sum_k \sum_j f(k-j)g(j) e^{-2i\pi(k-j)x/n} = \sum_k f(k-j) e^{-2i\pi(k-j)x/n} \times \sum_j g(j) e^{-2i\pi jx/n} \\ &= \sum_\ell f(\ell) e^{-2i\pi \ell x/n} \times \sum_j g(j) e^{-2i\pi jx/n} = \widehat{f}(x) \times \widehat{g}(x). \end{aligned}$$

1.41 We have

$$\begin{aligned} \mathcal{F}_{A+p}(x) &= \sum_{k \in (A+p)} e^{-2i\pi kx/n} = \sum_{\ell \in A} e^{-2i\pi(\ell+p)x/n} \\ &= e^{-2i\pi px/n} \sum_{\ell \in A} e^{-2i\pi \ell x/n} = e^{-2i\pi px/n} \mathcal{F}_A(x). \end{aligned}$$

If $\mathcal{F}_A(x) \neq 0$ this yields $e^{-2i\pi px/n} = 1$, i.e. $px/n \in \mathbb{Z}$.

2.38 Fig. 8.1 is an excerpt of a small composition.

2.41 The direct part uses the convolution product:



Fig. 8.1. The two hands play reverse intervals in two Z-related pc-sets

$$h = \frac{2}{n}(1, 1 \dots 1) - (1, 0, 0 \dots) = \frac{2}{n}\mathbf{1} - \delta.$$

Consider any hexachord A and its characteristic map $\mathbf{1}_A$:

$$h * \mathbf{1}_A = \frac{2}{n}\mathbf{1} * \mathbf{1}_A - \delta * \mathbf{1}_A = \frac{2\#A}{n}\mathbf{1} - \mathbf{1}_A = \mathbf{1} - \mathbf{1}_A$$

when $2\#A = n$, i.e. A is a generalised hexachord (it divides \mathbb{Z}_n in two parts of same size), and the map that we computed is 0 when $x \in A$ and 1 else, i.e. $h * \mathbf{1}_A$ is equal to the characteristic function $\mathbf{1}_{\mathbb{Z}_n \setminus A}$ of the complement of A .

To prove that h is a spectral unit we must study its eigenvalues. The matrix \mathcal{H} derives from the matrix $\mathbf{1}$ with only ones, whose nullspace has dimension $n - 1$ (the hyperplane $x_1 + \dots + x_n = 1$) and hence 0 is an eigenvalue with multiplicity $n - 1$. The other eigenvalue is n , associated with vector $(1, 1 \dots 1)$. Hence the eigenvalues of \mathcal{H} are

$$\frac{2}{n} \times 0 - 1 = -1 \quad \frac{2}{n} \times n - 1 = 1.$$

Both eigenvalues have magnitude 1; we have proved that h is a spectral unit, connecting any hexachord and its complement.

2.42 The Fourier coefficients of the spectral unit $j^3 = (0, 0, 0, 1, 0, 0, 0, 0, 0, 0, 0, 0)$ (i.e. the eigenvalues of its matrix) are $(1, -i, -1, i, 1, -i, -1, i, 1, -i, -1, i)$. Choosing arbitrarily cubic roots of each of the 12 coefficients yields cubic roots of j^3 , but most of these 531,441 distributions are irrational. One example (choosing the smallest phases for all cubic roots) is

$$\left(\frac{3}{8} + \left(\frac{1}{4} + \frac{i}{8} \right) \sqrt{3}, 0, 0, \frac{3}{8} - \frac{i\sqrt{3}}{8}, 0, 0, \frac{3}{8} - \left(\frac{1}{4} - \frac{i}{8} \right) \sqrt{3}, 0, 0, -\frac{1}{8} - \frac{i}{\sqrt{3}}, 8, 0, 0 \right).$$

To ensure *rational* spectral units, we must use Thm. 2.10, which determines all coefficients from the $\xi_d, d \mid n$. From it we get that $\xi_0 = +1$ (the case -1 is impossible), that for $d \in \{1, 2, 3, 6\}$, ξ_d is any power of $e^{2id\pi/12}$, and ξ_4 is a power of $e^{4i\pi/12}$; lastly, for any k coprime with 12, $\xi_{kd} = \xi_d^k$ (happily or by design, the last, complicated case will not occur in this exercise).

Since $\xi_1^3 = -i = e^{3i\pi/2}$ we have three choices: $\xi_1 \in \{e^{i\pi/2}, e^{7i\pi/6}, e^{11i\pi/6}\}$. The corresponding values of ξ_5, ξ_7, ξ_{11} are then determined (for instance $\xi_5 = \xi_1^5$). Similarly $\xi_2 \in \{-1, e^{5i\pi/3}, e^{i\pi/3}\}$ and hence $\xi_{10} = \overline{\xi_2}$.

The constraint of the theorem appears for ξ_3 which must be a power of i . The only possibility is then $\xi_3 = -i$ and $\xi_9 = i$; $\xi_4 \in \{1, j, j^2\} = \{1, e^{2i\pi/3}, e^{4i\pi/3}\}$ hence ξ_8 . Lastly $\xi_6 = -1$ and we are reduced to $3^3 = 27$ solutions, which can be produced by inverse DFT or matrix products (the amount of computation is the same).

A typical rational cubic root of j^3 is

$$\left(-\frac{1}{4}, \frac{1}{4}, 0, \frac{1}{4}, \frac{1}{4}, \frac{1}{2}, -\frac{1}{4}, \frac{1}{4}, 0, \frac{1}{4}, \frac{1}{4}, -\frac{1}{2}\right).$$

3.66 $\Phi_1 = X - 1, \Phi_2 = X + 1, \Phi_3 = X^2 + X + 1, \Phi_4 = X^2 + 1, \Phi_6 = X^2 - X + 1, \Phi_{12} = X^4 - X^2 + 1.$

3.67 $\Phi_{16}(X) = \frac{X^{16} - 1}{X^8 - 1} = X^8 + 1.$

3.69 Singular: by rote, there are as many odd and even elements, so $a_6 = 0.$

3.70 (CG) is the sum of all 6 fifths beginning on $C\sharp, D\sharp, F, G, A,$ and $B,$ minus the 5 fifths beginning on $D, E, F\sharp, G\sharp$ and $A\sharp.$

3.73 One could compute $\mathbf{A}(e^{2i\pi/30})$ numerically but this is not a rigorous proof (trigonometric computation is possible but deep). Best is to check that $\mathbf{A}(X)$ is divisible by $\Phi_{30}(X) = X^8 + X^7 - X^5 - X^4 - X^3 + X + 1.$ Polynomial division yields quotient $X^{16} - X^{15} + X^{14} + X^{11} + X^9 + X^7 + X^5 + X^3 + 1$ and remainder 0.

3.76 $\mathbf{A}(X) = (1 + X^5)(1 + X^8) = \frac{X^{10} - 1}{X^5 - 1}(1 + X^8) = \Phi_{10}\Phi_2\Phi_{16}.$

Hence $R_A = \{2, 10, 16\}$ (A tiles \mathbb{Z}_{16}).

4.56 Try multiplying the first line $(0, 1, 3, 8, 12, 18)$ by 2, 4, 8... Because of multipliers, there are three affine maps transforming each voice into another given one.

5.12 The smallest values of q satisfying the formula for $N = 100$ (i.e. both rational approximations are closer than $1/(10q)$) are $q = 36, 63, 70, 99, \dots$. For instance $\left(\frac{140}{99}, \frac{311}{99}\right) - (\sqrt{2}, \pi) \approx -(0.0000721, 0.000179),$ both coordinates well under $1/990.$

5.16 The proof follows the same pattern as the case developed in the example. Let $A = \{a_1, \dots, a_d\}$ be a d -subset of \mathbb{Z}_n (or indeed of the continuous circle modulo n) and $B = \{b_1, \dots, b_d\}$ be a subset of a regular d -polygon, i.e. $d(b_i - b_j) \in \mathbb{Z} \forall i, j,$ which is equivalent to $|\mathcal{F}_B(d)| = d$ as we have seen previously.

Assume B is the closest to A among similar subsets. Then by derivation

$$\frac{dAB^2}{db} = 2 \sum (b_k - a_k) = 0$$

where db stands for any db_i since they are differentially identical. If B is written as a particular type of subset of a polygon, e.g. $B = x + \{\dots b_0 + \frac{m_k}{d} \dots\}$ with a specific distribution of the integers $m_k,$ this pinpoints the value of the offset x (modulo n/d)

and hence of B , but this is not relevant in the following computation, insofar as we can assume that the quantities $b_k - a_k$ are small. We now compute the Fourier coefficient $\mathcal{F}_A(d)$:

$$\mathcal{F}_A(d) = \sum_k e^{-2i\pi d a_k/n} = \sum_k e^{-2i\pi d (b_k + (a_k - b_k))/n} = e^{-2i\pi d b/n} \sum_k e^{-2i\pi d (a_k - b_k)/n}$$

where b stands for any b_k , since $e^{-2i\pi d b_k/n}$ is independent of k by our assumption on the geometry of B .

Putting $\varphi_k = a_k - b_k$ one gets

$$|\mathcal{F}_A(d)| = \left| \sum_k e^{-2i\pi d/n \varphi_k} \right| = \left| \sum_k \left(1 - 2 \frac{\pi d}{n} \varphi_k - \frac{2\pi^2 d^2}{n^2} \varphi_k^2 + \dots \right) \right| \approx d - \frac{2\pi^2 d^2}{n^2} \sum_k \varphi_k^2$$

since $\sum \varphi_k = 0$. This yields the formula since $\sum_k \varphi_k^2 = VL^2$.

6.12

$$\begin{aligned} e^{-2i2\pi/12} - e^0 &= e^{-i\pi/3} (e^{-i\pi/3} - e^{+i\pi/3}) = -2i \sin \frac{\pi}{3} e^{-i\pi/3} \\ &= 2 \sin \frac{\pi}{3} e^{-i\pi/3 - i\pi/2} = \sqrt{3} e^{-5i\pi/3/6}. \end{aligned}$$

6.13 Between CEG and BDG the change is the same as between C and B. For a_3 it is $\Delta a_3 = e^{-2i3 \times 11\pi/12} - e^0 = i - 1 = \sqrt{2} e^{3i\pi/4}$.

However the phase of CEG is $\varphi_3 = 0.46365$ and for BEG it is 1.10715 ; hence the variation of phase is $\Delta \varphi_3 = 1.10715 - 0.46365 = 0.64350$. Similarly we find

$$\Delta a_5 = e^{-2i5 \times 11\pi/12} - e^0 = e^{10i\pi/12} - 1 = 2 \sin \frac{5\pi}{12} e^{5i\pi/12}$$

and $\Delta \varphi_5 = 1.83260 - 0.78540 = 1.04720$.

Notice that the phase of the difference Δa_k is not the difference of phases $\Delta \varphi_k$: the first is the direction of a vector in Hoffman's space ($\arg(a_k - b_k)$) and the second a difference of one coordinate in the torus of phases ($\arg(a_k) - \arg(b_k)$). This illustrates the fact that the map \arg is not linear.

6.14 $a_3 = 2$ and $a_5 = \frac{1}{2} + \frac{i\sqrt{3}}{2}$ so $\varphi_3 = 0, \varphi_5 = \pi/3$.

6.16 The inversion around 0 turns $\{0, 4, 7, 10\}$ into $\{0, 2, 5, 8\}$ (central symmetry $x \mapsto 12 - x$). A tentative motif between the minor seventh and the dominant seventh is given in Fig. 8.2 (I will readily agree that Wagner's version is better).



Fig. 8.2. Another Tristan chimera

8.2 Lewin's 'special cases'

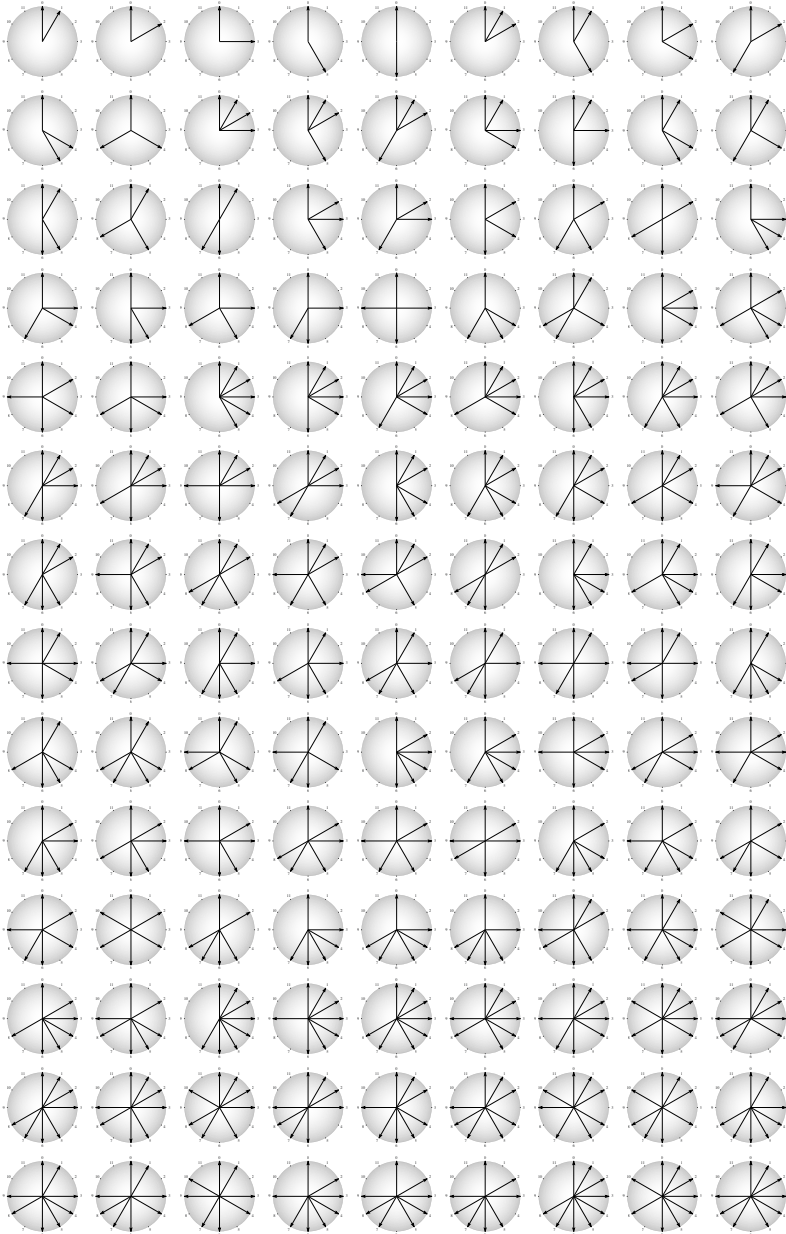


Fig. 8.3. Table of all classes of singular pc-sets

8.3 Some pc-sets profiles

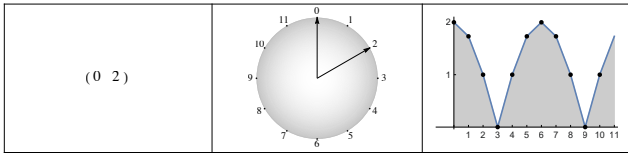


Fig. 8.4. Second/seventh

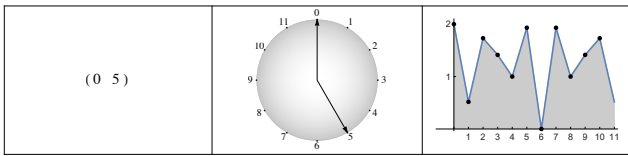


Fig. 8.5. Fourth/fifth

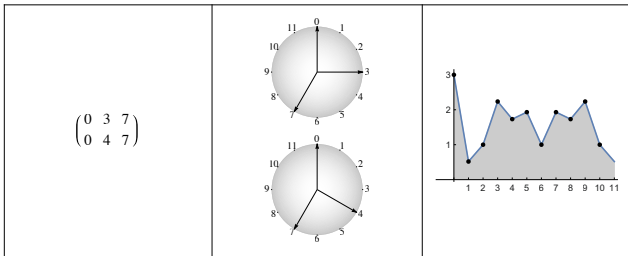


Fig. 8.6. Major/minor triad

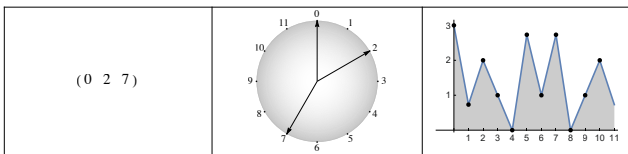


Fig. 8.7. Rock/blues bass

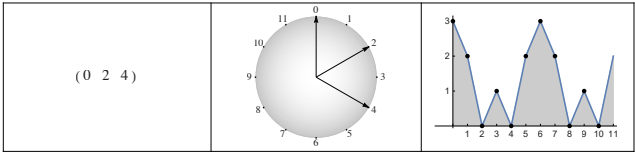


Fig. 8.8. Whole-tone trichord

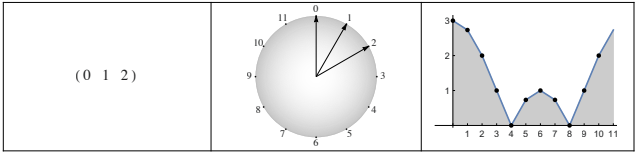


Fig. 8.9. Chromatic trichord

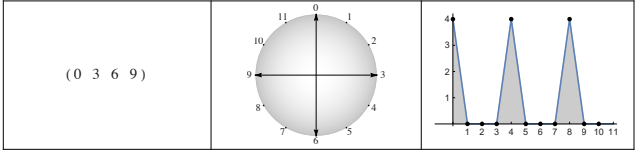


Fig. 8.10. Diminished seventh

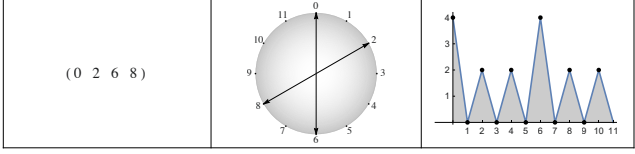


Fig. 8.11. Chunk of whole-tone scale

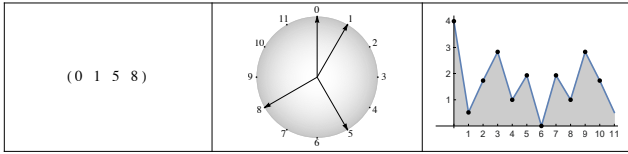


Fig. 8.12. S.N.C.F. jingle

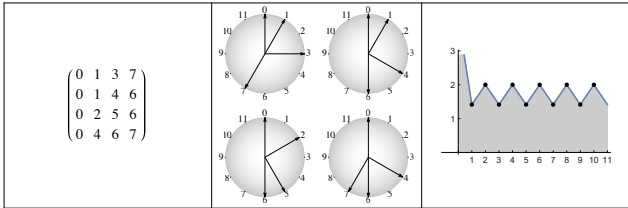


Fig. 8.13. Homometric quadruplet

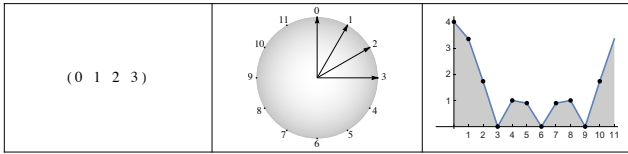


Fig. 8.14. Chromatic tetrachord

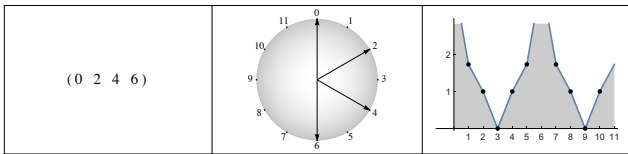


Fig. 8.15. Whole-tone tetrachord

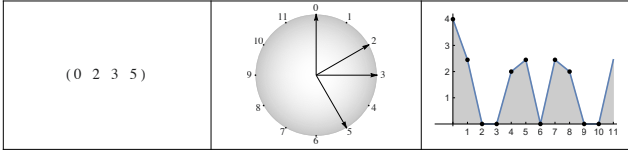


Fig. 8.16. An octa/diatonic tetrachord

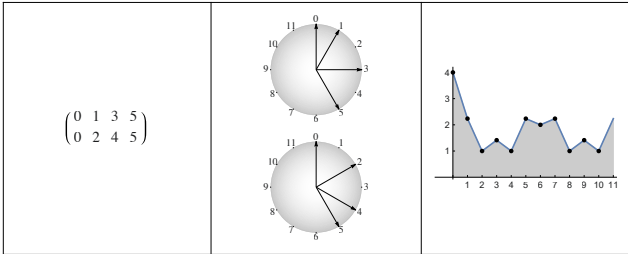


Fig. 8.17. A rather diatonic tetrachord

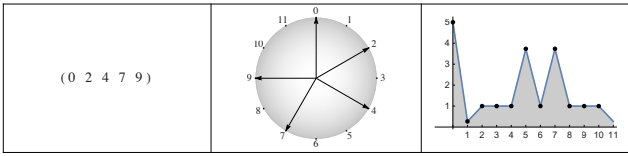


Fig. 8.18. Pentatonic scale

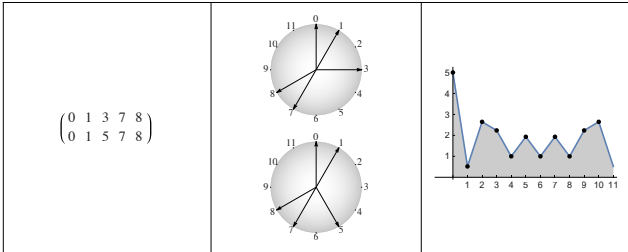


Fig. 8.19. Beginning of *La Puerta del Vino*

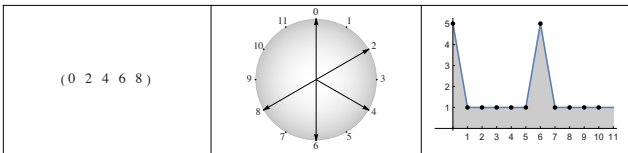


Fig. 8.20. Whole-tone pentachord

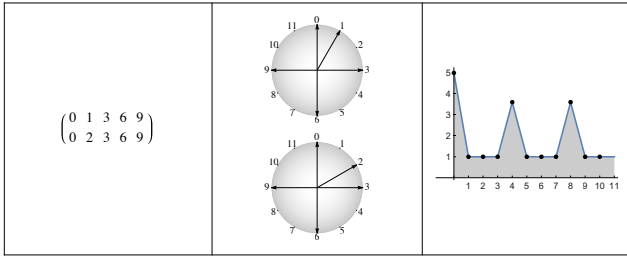


Fig. 8.21. A pentachord saturated in minor thirds

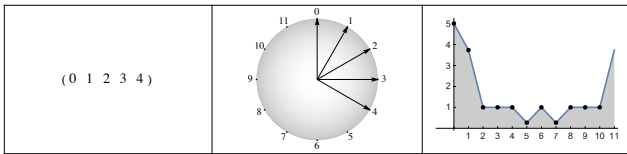


Fig. 8.22. Chromatic pentachord

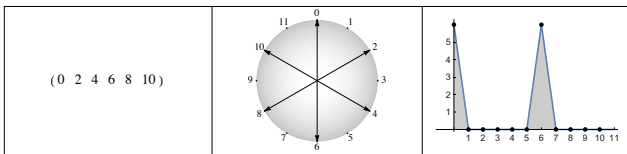


Fig. 8.23. Whole-tone scale

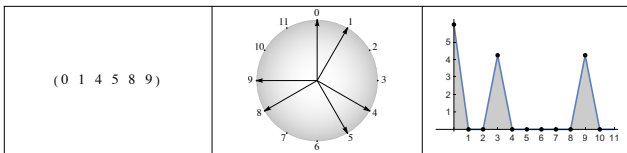


Fig. 8.24. Magic hexachord

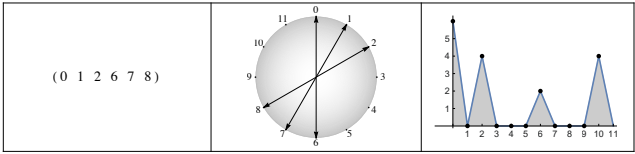


Fig. 8.25. Messiaen Mode M5

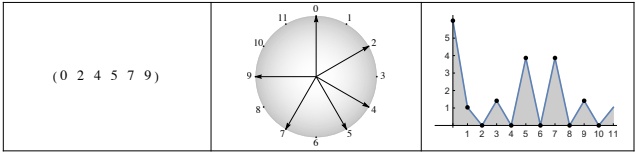


Fig. 8.26. Guidonian hexachord

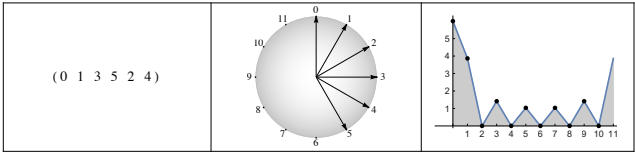


Fig. 8.27. Chromatic hexachord

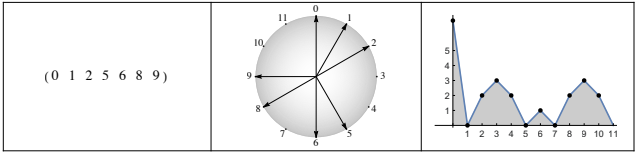


Fig. 8.28. Balanced seven-note scale

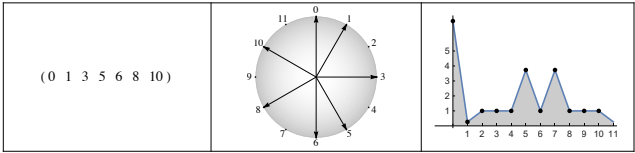


Fig. 8.29. Diatonic scale

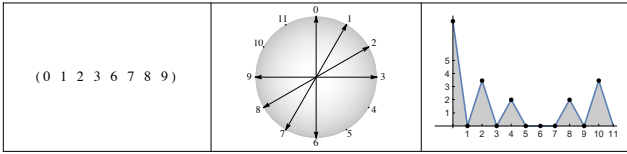


Fig. 8.30. Messiaen Mode M4

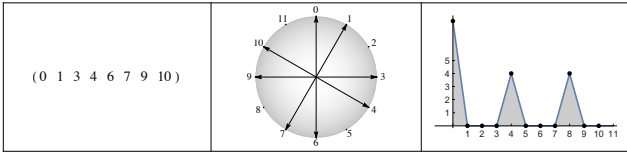


Fig. 8.31. Octatonic scale or M2

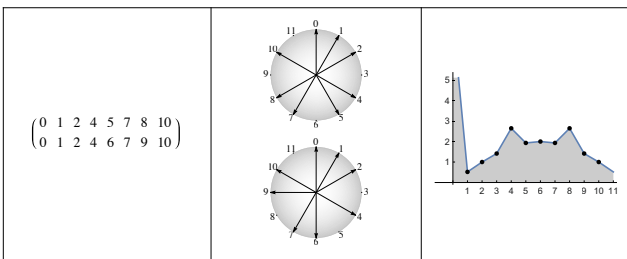


Fig. 8.32. An ‘octatonish’ collection in Stravinsky

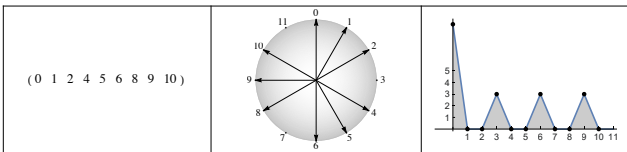


Fig. 8.33. Nonatonic scale or Messiaen Mode M3

8.4 Phases of major/minor triads







triad	θ_3	θ_5	triad	θ_3	θ_5
047 	0,46365	0,78540	2611 	2,67795	2,35619
058 	-0,46365	-0,78540	1610 	-2,67795	-2,35619
158 	-1,10715	-1,83260	037 	1,10715	-0,26180
169 	-2,03444	2,87979	2711 	2,03444	1,30900
269 	-2,67795	1,83260	038 	0,46365	-1,30900
2710 	2,67795	0,26180	148 	-0,46365	-2,87979
3710 	2,03444	-0,78540	149 	-1,10715	2,35619
3811 	1,10715	-2,35619	259 	-2,03444	0,78540
049 	-0,46365	1,30900	2510 	-2,67795	-0,26180
4811 	0,46365	2,87979	3610 	2,67795	-1,83260
1510 	-2,03444	-1,30900	3611 	2,03444	-2,87979
059 	-1,10715	0,26180	4711 	1,10715	1,83260

Fig. 8.34. Phase coordinates of major and minor triads

8.5 Very symmetrically decomposable hexachords

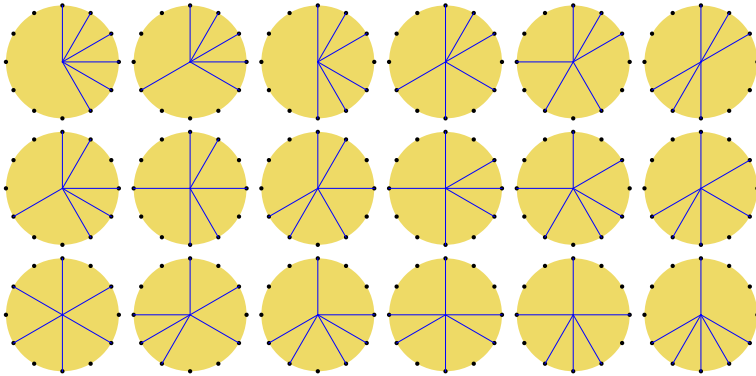


Fig. 8.35. The 18 most decomposable hexachords (up to transposition)

8.6 Major Scales Similarity

	MSS:	F	F#	G	G#	A	A#	B	C	C#	D	D#	E
Zarlino	59	0	112	204	316	386	498	590	702	814	884	1 017	1 088
MeanTone15	80	0	114	195	308	389	503	616	697	811	892	1 005	1 086
MeanTone16	117	0	110	196	306	392	502	612	698	807	894	1 004	1 090
WM2	120	0	82	196	294	392	498	588	694	784	890	1 004	1 086
Pythagore	142	0	114	204	294	408	498	612	702	816	906	996	1 110
Kirnberger2	147	0	90	204	294	386	498	590	702	792	895	996	1 088
Kirnberger3	164	0	90	195	294	386	498	590	698	792	890	996	1 088
Vallotti	164	0	94	196	298	392	502	592	698	796	894	1 000	1 090
WM1	181	0	90	192	294	390	498	588	696	792	888	996	1 092
Lindley94	224	0	108	200	305	402	502	606	699	807	901	1 004	1 104
WM3	235	0	96	204	300	396	504	600	702	792	900	1 002	1 098
WM5	235	0	108	210	306	408	504	612	708	804	912	1 008	1 110
BachLehman	260	0	104	200	306	404	502	604	698	808	902	1 004	1 104
WM4	268	0	91	196	298	395	498	595	698	793	893	1 000	1 097
Lehman94	283	0	94	202	298	399	500	596	700	796	900	1 000	1 097
Sparschu	293	0	105	204	301	404	498	605	702	804	904	1 000	1 105
Lindley	308	0	106	202	304	401	501	604	700	806	902	1 003	1 103
LindleyBis	362	0	97	201	297	400	499	598	701	796	901	997	1 099

Fig. 8.36. Values of MSS for different tunings

See the algorithm in Section 3.3 for computing the MSS of any other tuning.